

Asclepius: A Spectrum Evaluation Benchmark for Medical Multi-Modal Large Language Models

Jie Liu^{1*}, Wenxuan Wang^{2*}, Yihang Su³, Jingyuan Huan³, Yudi Zhang⁴, Cheng-Yi Li^{5,6},
Wenting Chen^{1†}, Xiaohan Xing⁷, Kao-Jung Chang^{5,6}, Linlin Shen⁴, Michael R. Lyu³

¹The City University of Hong Kong ²Renmin University of China

³The Chinese University of Hong Kong ⁴Shenzhen University

⁵National Yang Ming Chiao Tung University

⁶Taipei Veterans General Hospital ⁷Stanford University

Project Page: <https://github.com/ljwztc/Asclepius>

Abstract

The significant breakthroughs of Medical Multi-Modal Large Language Models (Med-MLLMs) renovate modern healthcare with robust information synthesis and medical decision support. However, these models are often evaluated on benchmarks that are unsuitable for the Med-MLLMs due to the complexity of real-world diagnostics across diverse specialties. To address this gap, we introduce Asclepius, a novel Med-MLLM benchmark that comprehensively assesses Med-MLLMs in terms of: distinct medical specialties (cardiovascular, gastroenterology, etc.) and different diagnostic capacities (perception, disease analysis, etc.). Grounded in 3 proposed core principles, Asclepius ensures a comprehensive evaluation by encompassing 15 medical specialties, stratifying into 3 main categories and 8 sub-categories of clinical tasks, and exempting overlap with existing VQA dataset. We further provide an in-depth analysis of 6 Med-MLLMs and compare them with 3 human specialists, providing insights into their competencies and limitations in various medical contexts. Our work not only advances the understanding of Med-MLLMs' capabilities but also sets a precedent for future evaluations and the safe deployment of these models in clinical environments.

1 Introduction

The advent of Multi-Modal Large Language Models (MLLMs), such as GPT-4V (OpenAI, 2023), Gemini (Team et al., 2023), LLaVA (Liu et al., 2023b), and MiniGPT-4 (Zhu et al., 2023), represents a significant stride towards artificial general intelligence due to their exceptional proficiency in tackling intricate tasks. These advancements have not only expanded the capabilities of models in natural scenes but have also paved the way

*J. Liu (♠ ♣ ♥), W. Wang (♥ ♣ ◇) make equal contribution. ♠: Conceptualization; ♥: Implementation; ♣: Writing; ◇: Visualization.

†Corresponding Author

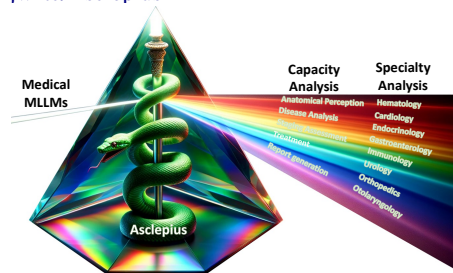


Figure 1: **Asclepius**, a spectrum evaluation benchmark for Med-MLLMs, analyzes models on the capacity dimension with 8 clinical tasks and the specialty dimension with 15 medical specialties.

for specialized enhancement in healthcare, as seen with the emergence of recent Medical Multi-modal Large Language Models (Med-MLLMs) (Moor et al., 2023a; Liu et al., 2023a; Lee et al., 2023; Zhang et al., 2023c).

Despite the promising advancements, the evaluation of these models relies predominantly on a limited set of samples (Wu et al., 2023a; Li et al., 2023b; Zhou et al., 2023; Moor et al., 2023a), which provides an incomplete picture of their capabilities. Current medical benchmarks, originally designed for traditional learning models, fall short in measuring the sophisticated capabilities of Med-MLLMs (Moor et al., 2023b; Li et al., 2023a). This misalignment highlights the necessity for comprehensive benchmarks that can systematically assess diverse perspectives of Med-MLLM. To this end, we propose a novel benchmark Asclepius that is akin to analyzing the spectrum of light with a prism, as illustrated in Figure 1.

Developing such a benchmark is challenging, especially in the medical field, due to the variation in practical expertise across different domains (Wang et al., 2023). For instance, a cardiologist may require a referral to a gastroenterologist when encountering conditions outside their primary domain of expertise due to the distinct specializations

Table 1: **Comparison of Med-MLLMs’ Datasets.** The Asclepius is categorized by both medical specialty and capability, encompassing 15 major specialties and 8 core competencies, and includes human specialists evaluation scores.

Name	Modality	Body parts and organs	Division		Original	Human Evaluation
			Specialty	Capacity		
ROCO (Pelka et al., 2018)	Radiology	/	✗	✗	✓	✗
VQA-RAD (Lau et al., 2018)	Radiology	3	✗	✗	✓	✗
SLAKE (Liu et al., 2021)	Radiology	5	✗	✗	✓	✗
PathVQA (He, 2021)	Pathology	/	✗	✗	✓	✗
MedMD (Wu et al., 2023b)	Radiology	17	✗	✗	✗	✗
PMC-VQA (Zhang et al., 2023c)	Multi-Modality	/	✗	✗	✗	✗
Asclepius	Multi-Modality	79	✓	✓	✓	✓

within each field (Forrest et al., 2000; Forrest and Reid, 2001). Traditional model evaluation methods often overlook the need for specialty-specific assessments, resulting in limited applicability and reliability in specialized medical contexts. This drives our approach to consider the variation in expertise across different medical specialties and to assess Med-MLLMs’ abilities in specialization-specific knowledge. Furthermore, the complex clinical decision-making processes, which involve perception, cognition, and reasoning (Lyman and Kuderer, 2023; Liberatore and Nydick, 2008; Patel et al., 2002; Kassirer and Gorry, 1978), present a second challenge. Med-MLLMs should have a diverse set of capabilities, such as interpreting medical imagery and understanding pathophysiology, to mimic these processes. Current evaluation frameworks (Lau et al., 2018; Pelka et al., 2018; Liu et al., 2021), which often focus on tasks like general radiology VQA, fail to precisely capture clinical performance. Thus, three core principles is proposed to address these concerns.

The philosophy to create Asclepius (1) *Multi-Specialty Coverage*: Our benchmark is meticulously designed to encompass a spectrum of 15 medical specialties. By systematically including questions from various specialties, such as cardiology, neurology, hematology, and endocrinology, the benchmark can evaluate the performance of Med-MLLMs in different medical domains. (2) *Multi-Dimensional Capacity*: Acknowledging the intricacies inherent in medical problem-solving, our benchmark is meticulously designed to evaluate a spectrum, divided into 3 main categories and 8 sub-categories. (3) *Original and Blindness*: The questions in MedVQABench are sourced from contemporary educational materials, medical examinations, and visual datasets, rather than integrating previously existing multiple VQA datasets, ensur-

ing the originality of our benchmark. Moreover, we have developed a website that allows submission and server-side evaluation of results to ensure integrity and fairness in the evaluation process.

In summary, our main contributions are summarized as follows:

- **Systematically-Constructed Dataset**: Our study introduces a meticulously crafted dataset designed to evaluate Med-MLLMs. This dataset encompasses a comprehensive range of 15 medical specialties, targeting 79 distinct body parts and organs. Furthermore, it is stratified into 3 main categories and 8 sub-categories, each corresponding to specific capacities within the medical domain.
- **Comprehensive Benchmarking**: Our study establishes a rigorous benchmark for the comprehensive assessment of 6 Med-MLLMs. In addition, 3 human doctors from varied specialties and levels of experience, ranging from junior to senior, answer the question to evaluate the human performance in this benchmark. This benchmark enables a direct comparison between Med-MLLMs and human specialists, providing valuable insights into the current state of AI in healthcare.
- **Analysis and Observations**: We provide several insights with corresponding suggestions (§5) based on evaluation results, shedding light on their strengths and weaknesses for Med-MLLMs.

2 Related Work

2.1 Medical Multi-Modal Large Language Models (Med-MLLMs)

The field of medicine frequently engages with diverse data modalities, including but not limited

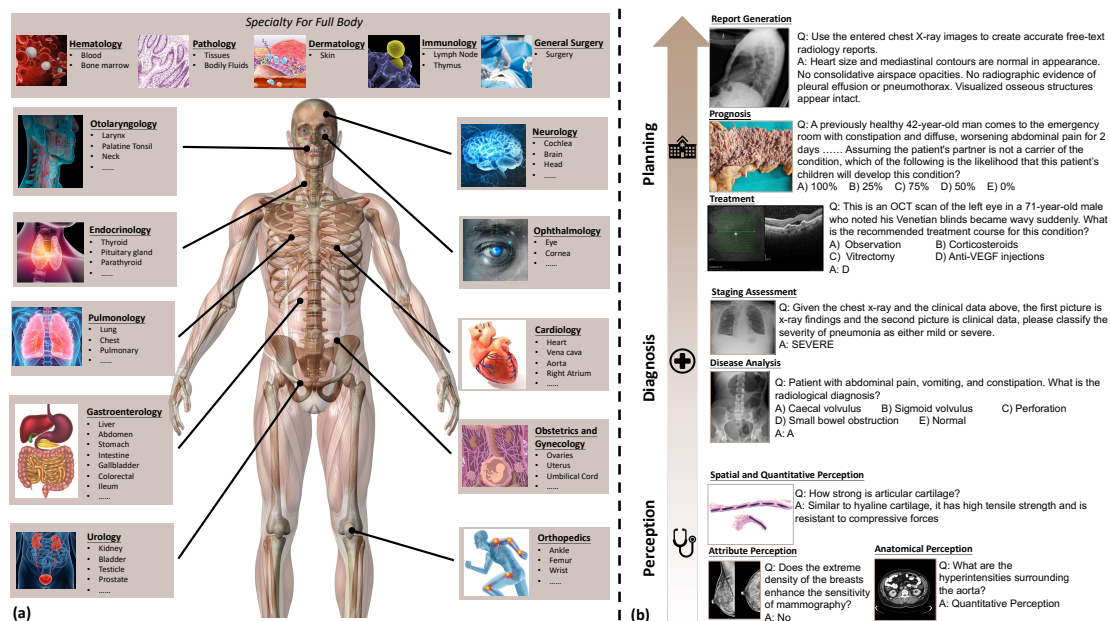


Figure 2: **Asclepius Overview.** (a) Involves 15 specialties and 79 body parts and organs in total, representing the critical component of the healthcare system. (b) Shows examples for 8 distinct capacities, offering a multifaceted evaluation of Med-MLLMs.

to text, computed tomography (CT) scans, dermoscopy images, and histopathological slides. In order to effectively replicate the complex decision-making processes of healthcare professionals, Medical Multi-Modal Large Language Models (Med-MLLMs) have been developed. Initial research efforts in this area have focused on the fusion of text with single medical imaging modalities (Liu et al., 2023a; Lee et al., 2023; Zhou et al., 2023; Thawkar et al., 2023; Wu et al., 2023b). These contributions laid the groundwork for subsequent advances in the field. Progressing further, recent studies have aimed to amalgamate a broader range of modalities (Belyaeva et al., 2023; Zhang et al., 2023a,c; Li et al., 2023a; Zhang et al., 2023b). In Asclepius, we thoroughly assess the capabilities of these models, particularly in terms of their performance in various specialties and capacities.

2.2 Benchmark for Med-MLLMs

In the rapidly evolving domain of Med-MLLMs, the development of benchmarks for evaluating these models is of paramount concern. Recent works (Zhang et al., 2023a; Belyaeva et al., 2023; Li et al., 2023a; Lu et al., 2023; Liu et al., 2023a) have endeavored to aggregate data from a variety of publicly available sources (Subramanian et al., 2020; Yang et al., 2023; Irvin et al., 2019; Johnson et al., 2019; He, 2021; Lau et al., 2018; Liu

et al., 2021) to create larger and more comprehensive datasets. Subsequently, ChatGPT is employed to assist in filtering the aggregated data to ensure quality control. For instance, the MedMD (Wu et al., 2023b) collected data from existing visual-language medical datasets, such as MIMIC-CXR (Johnson et al., 2019) and PMC-OA (Lin et al., 2023), within the radiology domain. Similarly, the PMC-VQA Dataset (Zhang et al., 2023c) utilizes ChatGPT to create a Visual Question Answering (VQA) dataset based on image-text pairings from PMC-OA (Lin et al., 2023). The recently proposed OmnimedVQA (Hu et al., 2024) and GMAI-MMBench (Chen et al., 2024a) also evaluates Med-MLLMs with single and multiple choice questions, which has been proved to be limited and biased (Li et al., 2024), and cannot assess the models' generative capabilities and align with real-world settings. We compare Asclepius with existing works in Table 1. Different from previous works, in this paper, we propose a novel Med-MLLMs benchmark Asclepius, which is mainly built based on existing medical textbooks and medical image datasets with various question types. We aim to establish a new standard for Med-MLLM evaluation that upholds the integrity of the assessment and delivers accurate reflection of a model's true capabilities in clinical environment.

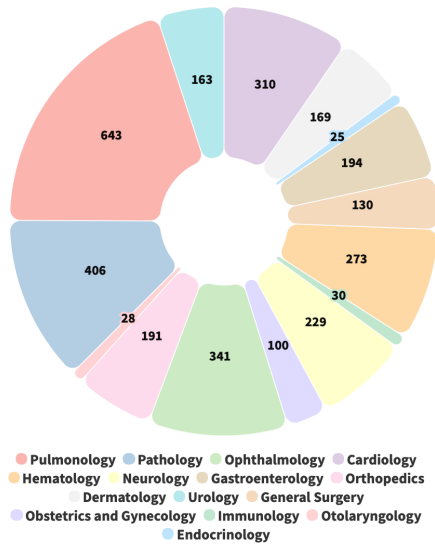


Figure 3: **Data Statistics for Specialty.** Currently, Asclepius incorporates 15 specialties with 3,232 multi-modal questions.

3 Asclepius Benchmark

Our Asclepius benchmark contains 3,232 original multi-modal questions, with a spectrum of 15 medical specialties and 8 capacities evaluation. This section is organized as follows: In Sec. 3.1 and Sec. 3.2, we discuss the design philosophy behind Asclepius and then present the specialty and capacity splitting. In Sec. 3.3, we details the question construction and provide statistics of Asclepius.

3.1 Multi-Specialty Coverage

Medical education is characterized by significant disparities in knowledge across different specialties, necessitating rigorous training for medical students within their chosen fields (Ledford et al., 2022; Davis, 2009). Analogously, Med-MLLMs developed to support clinical decision-making should exhibit a comparable depth of knowledge in their respective specialties to be effective. To this end, we include a diverse array of specialties. For specialties concerning specific organs, we incorporate *Cardiology*, *Endocrinology*, *Obstetrics and Gynecology*, *Gastroenterology*, *Urology*, *Orthopedics*, *Neurology*, *Otolaryngology*, *Pulmonology*, and *Ophthalmology*. In addition, for specialties encompassing full-body considerations, we include *Hematology*, *Pathology*, *Dermatology*, *Immunology*, and *General Surgery*. This diversified inclusion ensures that the Med-MLLMs reflect not only technological innovation but also practical utility within the routine operations of clinical practice.

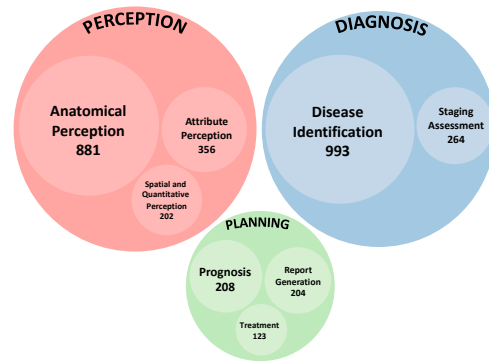


Figure 4: **Data Statistics for Capacities.** Asclepius includes two layers of capacity dimensions, which encompass 8 sub-capacities.

To provide a comprehensive view of the Med-MLLMs across these specialties, Figure 2 (a) offers an overview of the 15 specialties assessed in Asclepius. Each specialty represents a critical component of the healthcare system, addressing unique health concerns within its area of expertise. For additional information on the specialties included in this study, please refer to Appendix A.

3.2 Multi-Dimensional Capacity

The decision-making process in clinical practice is multifaceted and layered, encompassing a series of complex cognitive tasks (Liberatore and Nydick, 2008). The physician typically diagnoses the condition, assesses its stage, and then formulates a treatment plan and prognosis. Subsequently, these decisions and insights should be consolidated into a medical report. To mirror the decision-making intricacies in clinical settings, our benchmark incorporates three primary capacities for Med-MLLMs: *perception*, *diagnosis*, and *planning*. Furthermore, we have delineated secondary layer capacities to provide a more granular assessment. From *perception*, we derive (1) *anatomical perception*, (2) *attribute perception*, and (3) *spatial and quantitative perception*. From *diagnosis*, we extract (1) *disease analysis* and (2) *staging assessment*. Lastly, from *planning*, we have identified (1) *treatment*, (2) *prognosis*, and (3) *report generation*.

To illustrate the practical application of these capacities, Figure 2 (b) presents various case examples for each capacity within Asclepius. Asclepius currently encompasses 8 distinct sub-capacities, which offer a multifaceted evaluation of Med-MLLMs' performance in mimicking the decision-making process found in medical practice.

Please see Appendix C for details.

3.3 Data Collection

To create a comprehensive benchmark with a multi-faceted evaluation, our study needs to collect medical images and professional medical knowledge QA pairs, that can effectively test both specialties and capabilities of Med-MLLMs. Asclepius implements two strategies to generate these QA pairs. All the data collected in this work has necessary permissions and licenses for research use.

The first approach within Asclepius constructs QA pairs from pre-existing medical image datasets. We collected the test set of 10 different medical vision datasets to cover various question types (Liu et al., 2022; Kather et al., 2018; Tsuneki and Kanavati, 2021; Kumar et al., 2019; Yang et al., 2023; Shah, 2019; Acevedo et al., 2020; Holste et al., 2022; Kermany et al., 2018; Tschandl et al., 2018). Leveraging the collected datasets, we transformed the original image classification data into a VQA format. To augment the diversity of question types, we constructed several VQA templates for each dataset. For instance, the questions for DeepDRiD (Liu et al., 2022) were formulated as "What is the severity level of diabetic retinopathy in this retinal fundus image?", "Does the retinal fundus image show signs of diabetic retinopathy at Level 3?", and "Select the severity level that best describes the retinal fundus image." Regarding the choice options, we incorporated the true label and three other randomly selected classification labels as the multiple-choice options. These datasets are restructured into a VQA format, with binary classification tasks formulated as yes/no questions and multi-class classification tasks presented as multiple-choice queries.

Concurrently, the benchmark employs a second strategy, incorporating QA pairs with images derived from the United States Medical Licensing Examination (USMLE) and current medical textbooks (Katzung et al., 2004; Pawlina and Ross, 2018; Murray et al., 2015; Barrett, 2010; Kumar et al., 2014; Snell, 2010; Sickles and D’Orsi, 2016). The integration of this content ensures alignment with the rigorous standards required for medical licensure, establishing a high bar for the medical knowledge assessment of Med-MLLMs. We took questions accompanied by images from the US-MILE and medical textbook quiz. In instances where the question text contained explanations pertaining to the associated image, we omitted it to ensure that MLLM needs to rely on both textual

and visual information to answer the questions accurately.

Statistics. Asclepius comprises a total of 3,232 data samples, which span across 15 medical specialties and 8 distinct sub-capacities. The visualizations of these two statistics are exhibited in Figure 3 and 4. Moving forward, we will preserve a balanced distribution of questions that fulfill various evaluation dimensions.

Data Split. To maintain the integrity and the blindness of the evaluation benchmark, we divided Asclepius into development and test subsets. 100 questions are randomly selected as the development set that is entirely publicly accessible, with ground truth answers for each question. The random selection maintains consistent statistics of development and test sets. Conversely, the test subset is only partially disclosed, with data samples being publicly available without ground truth answers. To ascertain the performance on the test subset, participants are required to submit their predictions to the Asclepius server for an unbiased assessment.

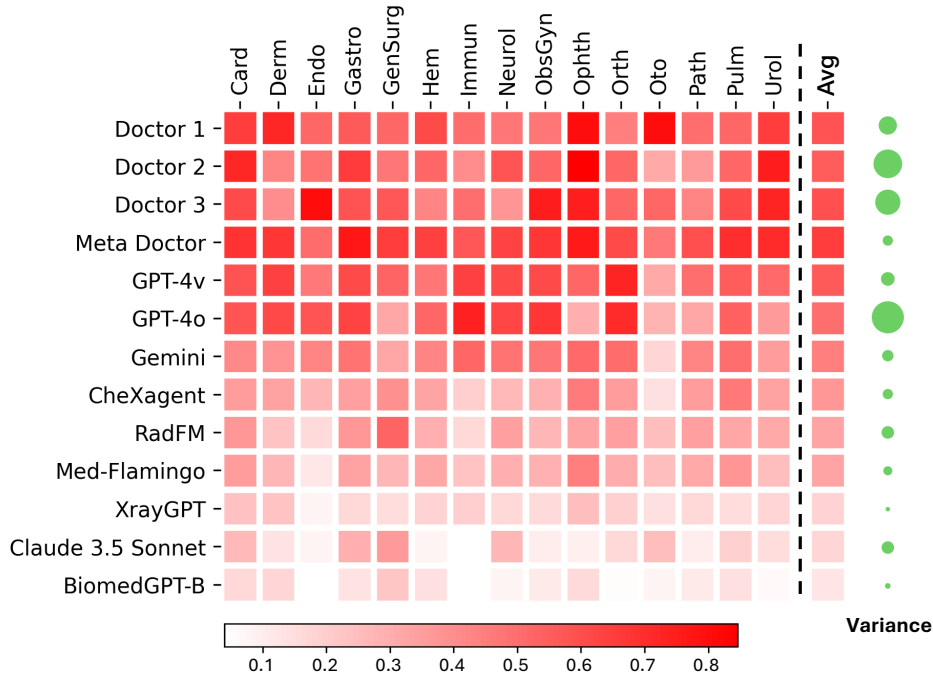
4 Experiments

4.1 Implementation

Model Evaluation. This benchmark focuses on four general MLLMs, namely GPT-4V (OpenAI, 2023), GPT-4o (OpenAI, 2024), Gemini (Team et al., 2023) and Claude 3.5 Sonnet (Claude, 2024), alongside five specialized Med-MLLMs: CheX-agent (Chen et al., 2024b), RadFM (Wu et al., 2023c), Med-Flamingo (Moor et al., 2023c), and XrayGPT (Thawkar et al., 2023), BiomedGPT-B (Zhang et al., 2024). The model information is shown in Appendix Table 5. The prompts for these MLLMs are in Appendix Table 6.

Human Study. To establish a benchmark for performance, the study also includes an evaluation of human specialists. Three clinical specialist doctors are selected to participate, who had expertise in certain medical specialties but were not good at all specialties. Specifically, Doctors 1 through 3 possess 4, 4, and 5 years of professional experience, respectively. Their confidence score for each specialty are listed in Appendix Table 4. Moreover, we also invited several doctors whose areas of expertise cover these 15 specialties, and we ensemble their results as the ideal case for meta doctors, who are all-powerful for all specialties.

Evaluation Metrics. Asclepius includes a range of question types: multiple choice, yes/no, open-



Abbreviation: Card (Cardiology), Derm (Dermatology), Endo (Endocrinology), Gastro (Gastroenterology), GenSurg (General Surgery), Hem (Hematology), Immun (Immunology), Neurol (Neurology), ObsGyn (Obstetrics and Gynecology), Ophth (Ophthalmology), Orth (Orthopedics), Oto (Otolaryngology), Path (Pathology), Pulm (Pulmonology), Urol (Urology).

Figure 5: **The spectrum of Med-MLLMs in Specialties.** Green circle size shows accuracy variance across specialties; larger circles indicate higher variance. Darker squares represent higher accuracy. Numeric details in Appendix Table 7. Meta doctor is ensembled from several doctors whose area of expertise cover these 15 specialties.

Table 2: **The Modality Study Result.** Full information means we use both textual and visual information. w/o means without.

Condition	Accuracy
Full information	46.2%
w/o image	32.0%
w/o text	23.9%

ended questions, and report generation tasks. We use accuracy for multiple-choice and yes/no questions and employ GPT to assess open-ended questions. Report generation is evaluated with the ROUGE-L score to measure alignment with gold-standard reports (Wu et al., 2023c; Chen et al., 2024b). Overall accuracy excludes report generation and is calculated as the ratio of correctly answered questions to the total applicable questions in benchmark. Please see Appendix G for details.

4.2 Visual and Textual Modality Study

To investigate the contribution of each modality, we conducted ablation experiments on GPT-4v. In the first group, we provided GPT-4v with only the visual information and the associated questions. Con-

versely, in the second group, we supplied GPT-4v with solely the textual information and the questions. The results are shown in Table 2. The accuracy decline observed for both groups when compared to the baseline condition with access to both modalities proves the importance of both textual and visual information for Asclepius benchmark. The models cannot answer the questions accurately by solely relying on either the text or visual information alone.

4.3 Results across Specialties

Our analysis reveals a broad spectrum of accuracy scores across the medical specialties in Figure 5. GPT-4V generally has the highest performance among the Med-MLLMs, with its average accuracy closest to human doctors. GPT-4o has the second-best performance among the Med-MLLMs, with moderate accuracy, but still significantly lower than GPT-4V. CheXagent, RadFM, Med-Flamingo, XrayGPT, and BiomedGPT show lower performance across all specialties. When comparing between Med-MLLMs and human doctors, human doctors generally outperform Med-MLLMs in all

Table 3: **The spectrum of Med-MLLMs in Capacity.** Avg* are the average accuracy of Anato, Attr, SpaQua, DisIde, Stag, Prog and Treat. Rep reports the ROUGE-L score. GPT-4V refuses to answer Rep question.

Model	Perception			Diagnosis		Planning			Avg*
	Anato	Attr	SpaQua	DisIde	Stag	Prog	Treat	Rep	
GPT-4V	0.462	0.542	0.599	0.592	0.504	0.649	0.556	N.A	0.558
GPT-4o	0.389	0.478	0.431	0.591	0.152	0.683	0.621	0.072	0.477
Gemini	0.410	0.410	0.460	0.386	0.523	0.654	0.323	0.082	0.452
CheXagent	0.297	0.334	0.337	0.326	0.451	0.519	0.315	0.157	0.368
RadFM	0.378	0.404	0.455	0.219	0.295	0.082	0.290	0.091	0.303
Med-Flamingo	0.313	0.312	0.272	0.259	0.439	0.394	0.161	0.133	0.307
Claude3.5Sonnet	0.196	0.160	0.322	0.060	0.061	0.101	0.161	0.051	0.136
XrayGPT	0.161	0.110	0.099	0.169	0.223	0.014	0.137	0.078	0.131
BiomedGPT-B	0.089	0.110	0.040	0.104	0.098	0.010	0.129	0.071	0.090
Doctor 1	0.541	0.368	0.700	0.590	0.667	0.500	0.733	N.A	0.586
Doctor 2	0.523	0.435	0.467	0.575	1.000	1.000	0.556	N.A	0.651
Doctor 3	0.517	0.480	0.700	0.624	0.538	1.000	0.429	N.A	0.613
Meta Doctor	0.581	0.589	0.593	0.686	0.605	1.000	0.772	N.A	0.689

Abbreviation: Anato (Anatomical Perception), Attr (Attribute Perception), DisIde (Disease Identification), Prog (Prognosis), SpaQua (Spatial and Quantitative Perception), Stag (Staging Assessment), Treat (Treatment Planning), Rep (Report Generation).

specialties. However, Med-MLLMs demonstrate a markedly lower variability in their performance across specialties when compared to humans.

4.4 Results across Capacities

The spectrum of Med-MLLMs in capacity is shown in Table 3. GPT-4V leads with the highest average accuracy across the seven tasks with an average score of 55.8%. This indicates that GPT-4V is likely the most versatile and reliable model for a range of medical tasks. Moreover, both GPT-4V and GPT-4o perform equally well in Disease Identification with a score of 59.2% and 59.1%, respectively, indicating strong capabilities in diagnosing diseases. Notably, GPT-4o achieves better performance than GPT-4V in prognosis and treatment planning with accuracy of 68.3% and 62.1%, suggesting its significant ability in planning tasks. As for the report generation task, GPT-4V refused to generate the responses (see Appendix F for details), which could be due to the model’s guidelines or limitations in this specific task. CheXagent has the highest ROUGE-L score for Report Generation at 0.157, although this is still relatively low, suggesting room for improvement in how these models generate medical reports.

5 Discussion

From the above results, six key insights have been deduced as follows:

1) Significant variance exists in different specialties. Human doctors have strong performances in certain specialties, but weaker performances in

others. As illustrated in Appendix Table 4, the confidence score assigned by Doctor2 is 5 for Cardiology compared to a score of 2 for Dermatology. Correspondingly, the results indicates that Doctor2 achieved a diagnostic accuracy of 71.4% for Cardiology, which markedly contrasts with a reduced accuracy of 40.0% for Dermatology. These variations highlight the complexity and diversity inherent to each medical specialty. Given these differences, it is critical to establish a comprehensive Med-MLLMs benchmark to systematically evaluate the performance across various specialties.

2) Human doctors outperform Med-MLLMs.

Human physicians surpass Med-MLLMs in diagnostic accuracy across all specialties. Even a junior doctor with an average accuracy of 57.4%, marginally exceeds the most proficient Med-MLLM, GPT-4V, which achieved an accuracy of 54.3%. This outcome suggests that, despite the advancements made in artificial intelligence, there is still a gap in diagnostic precision between human expertise and current Med-MLLMs. This underscores the need for continued development and specialization in the field of AI-driven medical diagnostics. On the other hand, the GPT-4V is comparable with junior human doctors, which indicates that Med-MLLMs like GPT-4V have the potential to complement the diagnostic process in practice. However, the current results indicate that the integration of such models into clinical workflows should be approached with caution, ensuring they serve as an adjunct to, rather than a replacement for, human clinical judgement.

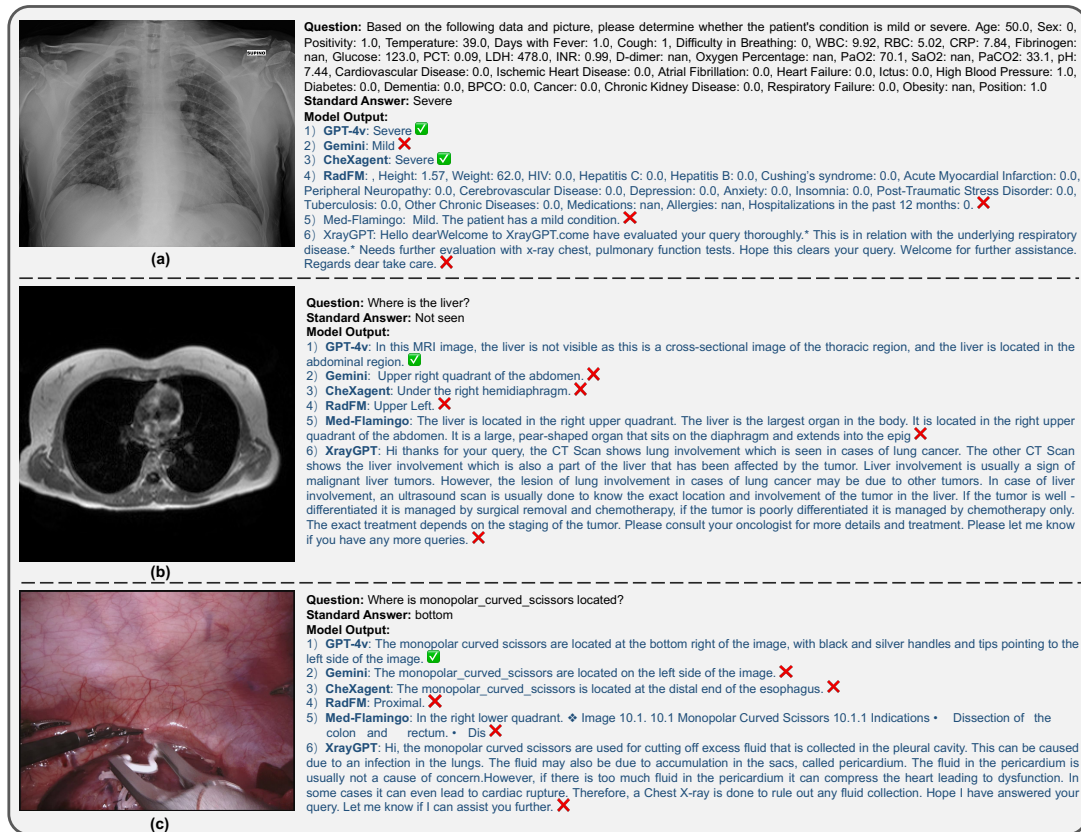


Figure 6: Case Study for Common Problem Revealed in Evaluation. (a) Case for Limited Instruction-following Capabilities. (b) Case for Failed Anatomical Perception. (c) Case for Failed Spatial and Quantitative Perception).

3) Superiority of Generalist MLLMs Over Specialized Med-MLLMs. Results reveal that generalist models such as GPT-4V and Gemini outperform five specialized Med-MLLMs in a dual-spectrum evaluation. Notably, RadFM, despite being trained on 16 million multi-modal medical question-answer pairs, remains inferior to GPT-4V. According to Appendix Table 5, the parameter count of the general MLLMs are much larger than that of Med-MLLMs. Therefore, we recommend that future research on Med-MLLMs should explore increasing the model parameter capacity to potentially improve their performance.

4) Limited Long-range Instruction Capture. Despite the implementation of careful prompt engineering, certain Med-MLLMs exhibit a tendency to generate indirect responses. Figure 6(a) illustrates instances where, instead of answering the condition as prompted, models like RadFM and XrayGPT provide irrelevant information. We argue that an optimal Med-MLLM should adhere to such detailed instructions.

5) Limited Multi-Modality Fusion. Figure 6 (b) illustrates the case that only GPT-4V accurately

incorporates image information into its response. In contrast, other Med-MLLMs simply restate the well-known fact that the liver is located in the upper right quadrant of the abdomen, neglecting to integrate the visual data presented. This pattern suggests a limited ability of most Med-MLLMs to synthesize image and text information, as they solely rely on textual prompts for their answers. Enhancing Med-MLLMs' multi-modal fusion capabilities emerges as a crucial and promising direction for future development.

6) Med-MLLMs offer the potential for integration of expansive and in-depth medical knowledge. In contrast to the wider variability observed among human physicians, Med-MLLMs exhibit more uniform performance, as depicted by the smaller green circles in Figure 5. This reduced variance signifies a standardized diagnostic capability of Med-MLLMs across different medical specialties. Such a pattern suggests that while human specialists are in-depth for particular domains, Med-MLLMs provide a more expansive knowledge across diverse medical fields, which could potentially be leveraged to augment clinical decision-

making processes. This is particularly relevant for complex multi-system disorders like hypermobile Ehlers-Danlos syndrome (hEDS), where an interdisciplinary approach is paramount (Gensemer et al., 2021). The advent of Med-MLLMs makes the integration of expansive and in-depth medical knowledge feasible, offering the potential to address the multifaceted needs of patients.

6 Conclusion

We introduce Asclepius, a comprehensive Med-MLLM evaluation benchmark with 3,232 multimodal questions spanning 15 medical specialties and 79 body parts/organs, for specialty and capacity analysis. It includes a website for secure server-side evaluation of submitted results. We assess 6 Med-MLLMs and 5 human doctors on Asclepius. Analysis shows that while current Med-MLLMs have limitations, they can supplement clinical judgment, suggesting potential for integrated medical knowledge application across breadth and depth.

7 Limitations

This paper has two primary limitations that offer avenues for future research:

- The current benchmark does not consider long patient history narratives that are often crucial for real-world clinical decision-making. As future work, we plan to expand the question set to incorporate queries that require comprehending and reasoning over long sequences of patient records. This will allow for a more comprehensive evaluation of Med-MLLMs' performance in scenarios that better approximate the complexities of actual clinical practice involving longitudinal patient data.
- The questions of Perception/Diagnosis/Planning are independent of each other currently, without coherence. Real clinical decision-making needs to be completed coherently from the front end to the back end. If one of them is wrong, the diagnosis will be not correct. In the future, the question sets will integrate long sequences of data in patient records and provide sequential disease questions for a patient.

Acknowledgments. This work was supported by the National Natural Science Foundation of China under Grant 82261138629 and 12326610.

References

- Andrea Acevedo, Anna Merino González, Edwin Santiago Alférez Baquero, Ángel Molina Borrás, Laura Boldú Nebot, and José Rodellar Benedé. 2020. A dataset of microscopic peripheral blood cell images for development of automatic recognition systems. *Data in brief*, 30(article 105474).
- Kim E Barrett. 2010. *Ganong's review of medical physiology*.
- Anastasiya Belyaeva, Justin Cosentino, Farhad Hormozdiari, Krish Eswaran, Shravya Shetty, Greg Corrado, Andrew Carroll, Cory Y McLean, and Nicholas A Furlotte. 2023. Multimodal llms for health grounded in individual-specific data. In *Workshop on Machine Learning for Multimodal Healthcare Data*, pages 86–102. Springer.
- Pengcheng Chen, Jin Ye, Guoan Wang, Yanjun Li, Zhongying Deng, Wei Li, Tianbin Li, Haodong Duan, Ziyang Huang, Yanzhou Su, et al. 2024a. Gmainbench: A comprehensive multimodal evaluation benchmark towards general medical ai. *arXiv preprint arXiv:2408.03361*.
- Zhihong Chen, Maya Varma, Jean-Benoit Delbrouck, Magdalini Paschali, Louis Blankemeier, Dave Van Veen, Jeya Maria Jose Valanarasu, Alaa Youssef, Joseph Paul Cohen, Eduardo Pontes Reis, et al. 2024b. Chexagent: Towards a foundation model for chest x-ray interpretation. *arXiv preprint arXiv:2401.12208*.
- Claude. 2024. <https://www.anthropic.com/news/claude-3-5-sonnet>. *Claude*.
- Dave A Davis. 2009. How to help professionals maintain and improve their knowledge and skills: Triangulating best practices in medicine. *Development of professional expertise: Toward measurement of expert performance and design of optimal learning environments*, pages 180–202.
- Christopher B Forrest, Gordon B Glade, Alison E Baker, Alison Bocian, Sarah von Schrader, and Barbara Starfield. 2000. Coordination of specialty referrals and physician satisfaction with referral care. *Archives of pediatrics & adolescent medicine*, 154(5):499–506.
- Christopher B Forrest and Robert J Reid. 2001. Prevalence of health problems and primary care physicians' specialty referral decisions. *Journal of family practice*, 50(5):427–427.
- Cortney Gensemer, Randall Burks, Steven Kautz, Daniel P Judge, Mark Lavalley, and Russell A Norris. 2021. Hypermobile ehlers-danlos syndromes: Complex phenotypes, challenging diagnoses, and poorly understood causes. *Developmental Dynamics*, 250(3):318–344.
- Xuehai He. 2021. Towards visual question answering on pathology images. In *Proceedings of the 59th*

- annual meeting of the association for computational linguistics and the 11th international joint conference on natural language processing*, volume 2.
- Gregory Holste, Song Wang, Ziyu Jiang, Thomas C Shen, George Shih, Ronald M Summers, Yifan Peng, and Zhangyang Wang. 2022. Long-tailed classification of thorax diseases on chest x-ray: A new benchmark study. In *MICCAI Workshop on Data Augmentation, Labelling, and Imperfections*, pages 22–32. Springer.
- Yutao Hu, Tianbin Li, Quanfeng Lu, Wenqi Shao, Junjun He, Yu Qiao, and Ping Luo. 2024. Omnimedvqa: A new large-scale comprehensive evaluation benchmark for medical lvlm. In *Proceedings of the IEEE/CVF Conference on Computer Vision and Pattern Recognition*, pages 22170–22183.
- Jeremy Irvin, Pranav Rajpurkar, Michael Ko, Yifan Yu, Silviana Ciurea-Ilcus, Chris Chute, Henrik Marklund, Behzad Haghgoo, Robyn Ball, Katie Shpanskaya, et al. 2019. Chexpert: A large chest radiograph dataset with uncertainty labels and expert comparison. *Proceedings of the AAAI conference on artificial intelligence*.
- Alistair EW Johnson, Tom J Pollard, Seth J Berkowitz, Nathaniel R Greenbaum, Matthew P Lungren, Chihying Deng, Roger G Mark, and Steven Horng. 2019. Mimic-cxr, a de-identified publicly available database of chest radiographs with free-text reports. *Scientific data*, 6(1):317.
- Jerome P Kassirer and G Anthony Gorry. 1978. Clinical problem solving: a behavioral analysis. *Annals of Internal Medicine*, 89(2):245–255.
- Jakob Nikolas Kather, Niels Halama, and Alexander Marx. 2018. [100,000 histological images of human colorectal cancer and healthy tissue](#).
- Bertram G Katzung, Todd W Vanderah, and Michael J Aminoff. 2004. Basic & clinical pharmacology.
- Daniel S Kermany, Michael Goldbaum, Wenjia Cai, Carolina CS Valentim, Huiying Liang, Sally L Baxter, Alex McKeown, Ge Yang, Xiaokang Wu, Fangbing Yan, et al. 2018. Identifying medical diagnoses and treatable diseases by image-based deep learning. *cell*, 172(5):1122–1131.
- Neeraj Kumar, Ruchika Verma, Deepak Anand, Yanning Zhou, Omer Fahri Onder, Efstratios Tsougenis, Hao Chen, Pheng-Ann Heng, Jiahui Li, Zhiqiang Hu, et al. 2019. A multi-organ nucleus segmentation challenge. *IEEE transactions on medical imaging*, 39(5):1380–1391.
- Vinay Kumar, Abul K Abbas, Nelson Fausto, and Jon C Aster. 2014. *Robbins and Cotran pathologic basis of disease, professional edition e-book*. Elsevier health sciences.
- Jason J Lau, Soumya Gayen, Asma Ben Abacha, and Dina Demner-Fushman. 2018. A dataset of clinically generated visual questions and answers about radiology images. *Scientific data*, 5(1):1–10.
- Christy Ledford, Esther Guard, Julie Phillips, Christopher Morley, Jacob Prunuske, and Andrea Wendling. 2022. How medical education pathways influence primary care specialty choice. *Family medicine*, 54(7):512–521.
- Seowoo Lee, Jiwon Youn, Mansu Kim, and Soon Ho Yoon. 2023. Cxr-llava: Multimodal large language model for interpreting chest x-ray images. *arXiv preprint arXiv:2310.18341*.
- Chunyuan Li, Cliff Wong, Sheng Zhang, Naoto Usuyama, Haotian Liu, Jianwei Yang, Tristan Naumann, Hoifung Poon, and Jianfeng Gao. 2023a. Llava-med: Training a large language-and-vision assistant for biomedicine in one day. *arXiv preprint arXiv:2306.00890*.
- Wangyue Li, Liangzhi Li, Tong Xiang, Xiao Liu, Wei Deng, and Noa Garcia. 2024. Can multiple-choice questions really be useful in detecting the abilities of llms? In *Proceedings of the 2024 Joint International Conference on Computational Linguistics, Language Resources and Evaluation (LREC-COLING 2024)*, pages 2819–2834.
- Yingshu Li, Yunyi Liu, Zhanyu Wang, Xinyu Liang, Lingqiao Liu, Lei Wang, Leyang Cui, Zhaopeng Tu, Longyue Wang, and Luping Zhou. 2023b. A comprehensive study of gpt-4v’s multimodal capabilities in medical imaging. *medRxiv*, pages 2023–11.
- Matthew J Liberatore and Robert L Nydick. 2008. The analytic hierarchy process in medical and health care decision making: A literature review. *European Journal of Operational Research*, 189(1):194–207.
- Weixiong Lin, Ziheng Zhao, Xiaoman Zhang, Chaoyi Wu, Ya Zhang, Yanfeng Wang, and Weidi Xie. 2023. Pmc-clip: Contrastive language-image pre-training using biomedical documents. *arXiv preprint arXiv:2303.07240*.
- Bo Liu, Li-Ming Zhan, Li Xu, Lin Ma, Yan Yang, and Xiao-Ming Wu. 2021. Slake: A semantically-labeled knowledge-enhanced dataset for medical visual question answering. In *2021 IEEE 18th International Symposium on Biomedical Imaging (ISBI)*, pages 1650–1654. IEEE.
- Fenglin Liu, Tingting Zhu, Xian Wu, Bang Yang, Chenyu You, Chenyang Wang, Lei Lu, Zhangdaihong Liu, Yefeng Zheng, Xu Sun, et al. 2023a. A medical multimodal large language model for future pandemics. *NPJ Digital Medicine*, 6(1):226.
- Haotian Liu, Chunyuan Li, Qingyang Wu, and Yong Jae Lee. 2023b. Visual instruction tuning. *arXiv preprint arXiv:2304.08485*.

- Ruhan Liu, Xiangning Wang, Qiang Wu, Ling Dai, Xi Fang, Tao Yan, Jaemin Son, Shiqi Tang, Jiang Li, Zijian Gao, et al. 2022. Deepdrid: Diabetic retinopathy—grading and image quality estimation challenge. *Patterns*, 3(6).
- Ming Y Lu, Bowen Chen, Drew FK Williamson, Richard J Chen, Kenji Ikamura, Georg Gerber, Ivy Liang, Long Phi Le, Tong Ding, Anil V Parwani, et al. 2023. A foundational multimodal vision language ai assistant for human pathology. *arXiv preprint arXiv:2312.07814*.
- Gary H Lyman and Nicole M Kuderer. 2023. Perception, cognition and thought: Part iii: Reasoning, judgement and decision-making.
- Michael Moor, Oishi Banerjee, Zahra Shakeri Hossein Abad, Harlan M Krumholz, Jure Leskovec, Eric J Topol, and Pranav Rajpurkar. 2023a. Foundation models for generalist medical artificial intelligence. *Nature*, 616(7956):259–265.
- Michael Moor, Qian Huang, Shirley Wu, Michihiro Yasunaga, Yash Dalmia, Jure Leskovec, Cyril Zakka, Eduardo Pontes Reis, and Pranav Rajpurkar. 2023b. Med-flamingo: a multimodal medical few-shot learner. In *Machine Learning for Health (ML4H)*, pages 353–367. PMLR.
- Michael Moor, Qian Huang, Shirley Wu, Michihiro Yasunaga, Cyril Zakka, Yash Dalmia, Eduardo Pontes Reis, Pranav Rajpurkar, and Jure Leskovec. 2023c. [Med-flamingo: A multimodal medical few-shot learner](#). ArXiv:2307.15189.
- Patrick R Murray, Ken S Rosenthal, and Michael A Pfaller. 2015. *Medical microbiology*. Elsevier Health Sciences.
- OpenAI. 2023. Gpt-4v(ision) system card. *OpenAI*.
- OpenAI. 2024. Gpt-4o(mni) system card. *OpenAI*.
- Vimla L Patel, David R Kaufman, and Jose F Arocha. 2002. Emerging paradigms of cognition in medical decision-making. *Journal of biomedical informatics*, 35(1):52–75.
- Wojciech Pawlina and Michael H Ross. 2018. *Histology: a text and atlas: with correlated cell and molecular biology*. Lippincott Williams & Wilkins.
- Obioma Pelka, Sven Koitka, Johannes Rückert, Felix Nensa, and Christoph M Friedrich. 2018. Radiology objects in context (roco): a multimodal image dataset. In *Intravascular Imaging and Computer Assisted Stenting and Large-Scale Annotation of Biomedical Data and Expert Label Synthesis: 7th Joint International Workshop, CVII-STENT 2018 and Third International Workshop, LABELS 2018, Held in Conjunction with MICCAI 2018, Granada, Spain, September 16, 2018, Proceedings 3*, pages 180–189. Springer.
- Arya Shah. 2019. [Breast ultrasound images dataset](#).
- Edward A Sickles and Carl J D’Orsi. 2016. Acr bi-rads®. *ACR BI-RADS®-Atlas der Mammadiagnostik: Richtlinien zu Befundung, Handlungsempfehlungen und Monitoring*, page 474.
- Richard S Snell. 2010. *Clinical neuroanatomy*. Lippincott Williams & Wilkins.
- Sanjay Subramanian, Lucy Lu Wang, Sachin Mehta, Ben Bogin, Madeleine van Zuynen, Sravanthi Parasa, Sameer Singh, Matt Gardner, and Hannaneh Hajishirzi. 2020. Medcat: A dataset of medical images, captions, and textual references. *arXiv preprint arXiv:2010.06000*.
- Gemini Team, Rohan Anil, Sebastian Borgeaud, Yonghui Wu, Jean-Baptiste Alayrac, Jiahui Yu, Radu Soricut, Johan Schalkwyk, Andrew M Dai, Anja Hauth, et al. 2023. Gemini: a family of highly capable multimodal models. *arXiv preprint arXiv:2312.11805*.
- Omkar Thawkar, Abdelrahman Shaker, Sahal Shaji Mulpilly, Hisham Cholakkal, Rao Muhammad Anwer, Salman Khan, Jorma Laaksonen, and Fahad Shahbaz Khan. 2023. Xraygpt: Chest radiographs summarization using medical vision-language models. *arXiv preprint arXiv:2306.07971*.
- Philipp Tschandl, Cliff Rosendahl, and Harald Kittler. 2018. The ham10000 dataset, a large collection of multi-source dermatoscopic images of common pigmented skin lesions. *Scientific data*, 5(1):1–9.
- Masayuki Tsuneki and Fahdi Kanavati. 2021. [Patchgas-tricadc22](#).
- USMLE. [United States Medical Licensing Examination](#).
- Dequan Wang, Xiaosong Wang, Lilong Wang, Mengzhang Li, Qian Da, Xiaoqiang Liu, Xiangyu Gao, Jun Shen, Junjun He, Tian Shen, et al. 2023. Medfmc: A real-world dataset and benchmark for foundation model adaptation in medical image classification. *arXiv preprint arXiv:2306.09579*.
- Chaoyi Wu, Jiayu Lei, Qiaoyu Zheng, Weike Zhao, Weixiong Lin, Xiaoman Zhang, Xiao Zhou, Ziheng Zhao, Ya Zhang, Yanfeng Wang, et al. 2023a. Can gpt-4v (ision) serve medical applications? case studies on gpt-4v for multimodal medical diagnosis. *arXiv preprint arXiv:2310.09909*.
- Chaoyi Wu, Xiaoman Zhang, Ya Zhang, Yanfeng Wang, and Weidi Xie. 2023b. Towards generalist foundation model for radiology. *arXiv preprint arXiv:2308.02463*.
- Chaoyi Wu, Xiaoman Zhang, Ya Zhang, Yanfeng Wang, and Weidi Xie. 2023c. Towards generalist foundation model for radiology.
- Jiancheng Yang, Rui Shi, Donglai Wei, Zequan Liu, Lin Zhao, Bilian Ke, Hanspeter Pfister, and Bingbing Ni. 2023. Medmnist v2-a large-scale lightweight benchmark for 2d and 3d biomedical image classification. *Scientific Data*, 10(1):41.

- Kai Zhang, Jun Yu, Zhiling Yan, Yixin Liu, Eashan Adhikarla, Sunyang Fu, Xun Chen, Chen Chen, Yuyin Zhou, Xiang Li, et al. 2023a. Biomedgpt: A unified and generalist biomedical generative pre-trained transformer for vision, language, and multimodal tasks. *arXiv preprint arXiv:2305.17100*.
- Kai Zhang, Rong Zhou, Eashan Adhikarla, Zhiling Yan, Yixin Liu, Jun Yu, Zhengliang Liu, Xun Chen, Brian D Davison, Hui Ren, et al. 2024. A generalist vision–language foundation model for diverse biomedical tasks. *Nature Medicine*, pages 1–13.
- Wenxuan Zhang, Sharifah Mahani Aljunied, Chang Gao, Yew Ken Chia, and Lidong Bing. 2023b. M3exam: A multilingual, multimodal, multilevel benchmark for examining large language models. *arXiv preprint arXiv:2306.05179*.
- Xiaoman Zhang, Chaoyi Wu, Ziheng Zhao, Weixiong Lin, Ya Zhang, Yanfeng Wang, and Weidi Xie. 2023c. Pmc-vqa: Visual instruction tuning for medical visual question answering. *arXiv preprint arXiv:2305.10415*.
- Juexiao Zhou, Xiaonan He, Liyuan Sun, Jiannan Xu, Xiuying Chen, Yuetan Chu, Longxi Zhou, Xingyu Liao, Bin Zhang, and Xin Gao. 2023. Skingpt-4: an interactive dermatology diagnostic system with visual large language model. *arXiv preprint arXiv:2306.00890*.
- Deyao Zhu, Jun Chen, Xiaoqian Shen, Xiang Li, and Mohamed Elhoseiny. 2023. Minigpt-4: Enhancing vision-language understanding with advanced large language models. *arXiv preprint arXiv:2304.10592*.

Appendix for Asclepius

Abstract. In this supplementary material, we provide additional information about the Asclepius. Appendix A illustrates the definition of each specialty. Appendix B provides list of involved organ. Appendix C elaborates on the capacity taxonomy. In Appendix D, we provide some examples in Asclepius and some case studies of Med-MLLMs for each capacity. Finally, Appendix E supplements the qualitative and quantitative results in the main paper, including the visualization of statistics for specialty and capacity, and the digital results of different specialties.

A Specialty List

Asclepius encompasses 15 medical specialties that represent the core divisions of modern healthcare. These specialties can be broadly categorized into several groups based on their focus areas and interconnected nature. They are Hematology, Cardiology, Endocrinology, Obstetrics and Gynecology, Gastroenterology, Immunology, Urology, Orthopedics, Neurology, Otolaryngology, Pulmonology, Dermatology, Pathology, Ophthalmology, General surgery.

Internal Medicine Specialties: *Cardiology* focuses on the heart and cardiovascular system, diagnosing and treating various heart conditions. *Pulmonology* addresses disorders of the respiratory system, including the lungs and airways. *Gastroenterology* specializes in the digestive system, managing disorders from the esophagus to the intestines. *Endocrinology* deals with the endocrine system and hormone-related disorders, while *Hematology* focuses on blood, blood-forming organs, and related diseases. *Immunology* studies the immune system and its disorders, playing a crucial role in understanding the body's defense mechanisms.

Surgical and Procedural Specialties: *General Surgery* encompasses procedures involving abdominal organs, endocrine glands, and various soft tissues. *Orthopedics* concentrates on the musculoskeletal system, treating bone, joint, and muscle disorders. *Urology* addresses both the urinary tract and male reproductive system. *Otolaryngology* (ENT) specializes in ear, nose, and throat conditions, while *Ophthalmology* focuses exclusively on eye diseases and vision care.

Specialized Care and Diagnostics: *Obstetrics and Gynecology* provides comprehensive care for

women's reproductive health and pregnancy. *Dermatology* focuses on conditions affecting the skin, hair, and nails. *Neurology* addresses disorders of the nervous system, including the brain and spinal cord. *Pathology*, serving as a diagnostic cornerstone, studies disease processes through tissue and fluid examination.

B Organ list

This section we list the involved body parts and organs in this benchmark.

53 Body Parts: Abdomen, Neck, Chest, Head, Cervical Vertebrae, Ankle, Femur, Vertebrae, Bowel, Mandible, Knee, Cochlea, Hand, Bladder, Spine, Wrist, Pelvis, Carotid Artery, Carotid Bifurcation, Trachea, Larynx, Colorectal, Blood, Forearm, Elbow, Hip, Muscle, Reproductive Systems, Gastrointestinal Tract, Ligamentum Nuchae, Small Intestine, Colon, Seminal Vesicle, Duodenum, Anterior Pituitary, Parathyroid, Vena-cava, Right Atrium, Left Ventricle, Muscular Artery, Bronchiole, Aorta, Palatine Tonsil, Pyloric Stomach, Cardiovascular, Endocrine, Musculo skeletal, Ophthalmic, Pulmonary, Blood smear, Cartilage, Adipose Tissue, Tendon, Nervous Tissue,

26 Organs: Liver, Lung, Brain, Breast, Testicle, Thyroid, Ovaries, Kidney, Heart, Uterus, Intestine, Pancreas, Pituitary gland, Stomach, Gallbladder, Skin, Eye, Blood, Ileum, Lymph Node, Umbilical Cord, Prostate, Duodenum, Parathyroid, Esophagus, Appendix

C Capacity

C.1 Perception

C.1.1 Anatomical Perception

Anatomical Perception is the ability to recognize and understand the normal structures of the body, including their locations, sizes, shapes, and the planes in which they are imaged.

Anatomical Perception is foundational to medical imaging analysis, as it allows for the accurate identification of body parts and serves as a basis for detecting abnormalities. It involves discerning the detailed anatomy within complex images and is essential for any subsequent diagnostic or therapeutic action.

C.1.2 Attribute Perception

Attribute Perception is the capacity to discern various attributes of tissues and structures, such as their density, texture, composition, and presence of

pathological signs, along with recognizing instruments, modalities, and colors when applicable.

Attribute Perception focuses on the finer details that characterize tissues and help differentiate between normal and abnormal findings. It is vital for quality imaging interpretation and aids in the detailed understanding of pathologies and their implications on health.

C.1.3 Spatial and Quantitative Perception

Spatial and Quantitative Perception encompasses the skill to evaluate the spatial relations and quantitative aspects within medical images, such as counting entities and understanding their three-dimensional positions and relationships.

Spatial and Quantitative Perception is crucial for tasks that require an understanding of the geometry and distribution of anatomical structures and pathological findings, which is important for accurate diagnosis, surgical planning, and treatment evaluation.

C.2 Diagnosis

C.2.1 Disease Analysis

Disease Analysis is the ability to accurately detect and diagnose diseases from medical data, which may include imaging, laboratory results, patient history, and physical examination findings.

Disease Identification is the cornerstone of clinical practice, where the model's prowess in recognizing patterns and correlating them with potential diseases is essential. This involves not only identifying the presence of a disease but also understanding its nature.

C.2.2 Staging Assessment

Staging Assessment is the process of determining the extent or severity of a disease, especially cancer, within the body, which is crucial for choosing the most appropriate treatment strategy.

Staging Assessment evaluates how far a disease has progressed and is a critical step in the treatment planning process. It requires a comprehensive analysis of data to accurately classify the stage, which can significantly affect prognosis and treatment choices.

C.3 Planning

C.3.1 Treatment

Treatment is the selection and administration of the appropriate therapeutic interventions tailored to the individual patient's disease and condition.

The Treatment aspect involves creating a detailed plan for managing the patient's condition, which may include medication, surgery, lifestyle changes, or other therapies. The objective is to select the most effective and least invasive treatment options while considering the patient's preferences and overall health status.

C.3.2 Prognosis

Prognosis is the prediction of the likely course and outcome of a disease, taking into account the nature of the disease, the patient's general physical condition, and the treatment options available.

Prognosis is about looking ahead to predict possible outcomes for the patient. This includes estimating survival rates, potential complications, and the likelihood of disease recurrence. It is a vital part of patient counseling and informs decision-making for both clinicians and patients.

C.3.3 Report generation

Report generation is the synthesis of medical data and analytical findings into coherent, standardized, and actionable reports for use by healthcare providers.

Report Generation combines all the collected information into a format that is understandable and useful for guiding clinical decisions. It ensures that the insights gained from the model's analysis are communicated effectively, serving as a bridge between the model's output and clinical action steps.

D Examples in Asclepius

In Figures 7 to 11, we illustrate several examples in different specialties in Asclepius. Also, we provide some case studies for various capacities in Figures 12 to 14.

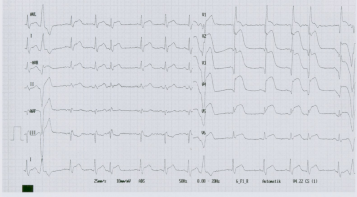
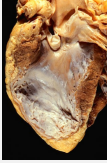
E Qualitative and Quantitative Results

This section supplements the results of evaluation:

Table 4 shows the confidence of doctors in various specialties.

We performed ablation experiments on GPT-4v to assess each modality's contribution. One group receives only visual information and questions, while another receives only text and questions. As shown in Appendix Table 2, both groups' accuracy decline compared to the baseline with both modalities, highlighting the necessity of combining textual and visual information for the Asclepius benchmark. Models cannot accurately answer questions using only text or visual data alone.

Cardiology

Question: A 57-year-old man is brought to the emergency department for crushing substernal chest pain at rest for the past 2 hours. The pain began gradually while he was having an argument with his wife and is now severe. He does not take any medications. He has smoked one pack of cigarettes daily for 35 years. He is diaphoretic. His temperature is 37.1°C (98.8°F), pulse is 110/min, respirations are 21/min, and blood pressure is 115/65 mm Hg. Pulse oximetry on room air shows an oxygen saturation of 97%. Cardiac examination shows an S4 gallop. The lungs are clear to auscultation. An ECG is shown. Which of the following is the most likely underlying cause of this patient's condition?

A) Occlusion of the right coronary artery
 B) Inflammation of the pericardium
 C) Occlusion of the left anterior descending artery
 D) Thromboembolism to the right interlobar pulmonary artery
 E) Diffuse coronary vasospasm
 F) Occlusion of the left circumflex artery
 G) Tear in the intimal lining of the aorta

Standard Answer: C) Occlusion of the left anterior descending artery


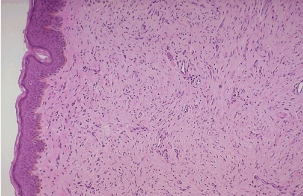
Question: A 65-year-old man has had increasing dyspnea and orthopnea for the past year. On physical examination there are rales in all lung fields. A chest x-ray shows cardiomegaly and pulmonary edema. An echocardiogram shows reduced cardiac output. The gross appearance of his heart shown here is most consistent with which of the following underlying conditions?

A) Amyloidosis
 B) Systemic hypertension
 C) Diffuse scleroderma
 D) Atherosclerosis
 E) Viral myocarditis

Standard Answer: D) Atherosclerosis

Figure 7: Examples for Cardiology.

Dermatology

Question: A 10-year-old child complains of intense itching of his hands. Physical examination reveals several linear gray-brown lesions a few millimeters in length that appear in the skin between his fingers. Some of these lesions have been excoriated by scratching. The finding from scraping these lesions is shown here. Which of the following infectious agents is the most likely cause?

A) Epidermophyton floccosum
 B) Herpes zoster
 C) Sarcoptes scabiei
 D) Staphylococcus aureus
 E) Malassezia furfur
 F) Papillomavirus

Standard Answer: C) Sarcoptes scabiei

Question: A 25-year-old man has multiple firm nodules, some of which are up to 1 cm in size, that are disfiguring because they are located on his hands and arms. Also noted on physical examination are scattered light brown macules with smooth borders, averaging about 2 to 3 centimeters in size, over the skin of his trunk and arms. The microscopic appearance of one of the nodular lesions is seen here. His father and brother have similar lesions. Which of the following is the most likely diagnosis?

A) Neurofibromatosis
 B) Kaposi sarcoma
 C) Nevocellular nevus
 D) Actinic keratosis
 E) Impetigo

Standard Answer: A) Neurofibromatosis

Figure 8: Examples for Dermatology.

As shown in Table 7, the human doctors' performance varies widely across specialties and individuals, with accuracy scores ranging from 0.286 to 0.846 in the different fields. The average accuracy of human doctors (calculated from the "Avg" column) ranges from 0.538 to 0.641, with Meta-Doctor having the highest average accuracy. Comparing the Med-MLLMs to human doctors, all the Med-MLLMs have a lower average accuracy than the human doctors. Among the Med-MLLMs, GPT-4V's performance is closest to that of human doctors, which surpasses Doctor2 by a small margin with an accuracy of 0.005.

Figure 15 visualizes the performance comparison of Med-MLLMs on the benchmark. Each model has its strengths and weaknesses, with GPT-4V showing the most robust performance across most areas. Gemini seems to be a decent second choice, particularly in prognosis. The other models have niche areas where they perform well but are

generally outperformed by the top two models.

F Evaluation Models

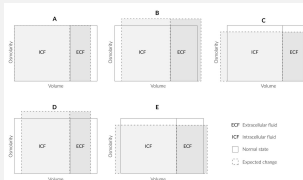
Asclepius focuses on four general MLLMs, including GPT-4V, GPT-4o, Gemini and Claude 3.5 Sonnet, along with five specialized Med-MLLMs, i.e. CheXagent, RadFM, Med-Flamingo, XrayGPT, and BiomedGPT, as shown in Table 5. We evaluate the GPT-4V, GPT-4o, Gemini and Claude 3.5 Sonnet through the official API. We test the rest of the specialized Med-MLLMs through the released code and pre-trained model. The prompt for these MLLMs are listed in Table 6, where the prompts for five Med-MLLMs are recommended in their papers. Sometimes GPT-4V may refuse to generate response. For example, GPT-4V generated 'I'm sorry, but I cannot provide the service of generating radiology reports. If you have any other questions or need information on a different topic, feel free to ask.'

Endocrinology

Question: A 32-year-old woman comes to the physician for increasing fatigue over the past 3 months. During this period, her appetite has decreased and she has lost 10 kg (22 lb). She also reports decreased sexual desire. She has a history of type 1 diabetes. Her pulse is 105/min and blood pressure is 95/63 mm Hg. Physical examination shows darkening of the skin and oral mucous membranes. Serum studies show: Na⁺ 130 mEq/L; K⁺ 5.2 mEq/L; Glucose (fasting) 74 mg/dL. Which of the following changes to body fluid volume and osmolality would most likely be expected?

A) A
B) B
C) C
D) D
E) E

Standard Answer: C) C



Question: A 23-year-old woman comes to physician for an annual health maintenance examination. She feels well. She is 155 cm (5 ft 1 in) tall and weighs 79 kg (174 lb); BMI is 33 kg/m². Examination shows a skin rash over both axillae. A photograph of her left axilla is shown. This patient's skin finding is most likely associated with which of the following conditions?

A) Niacin deficiency
B) Gastric malignant lymphoma
C) Primary adrenal insufficiency
D) Polycystic ovary syndrome
E) Hashimoto thyroiditis
F) Pregnancy

Standard Answer: D) Polycystic ovary syndrome





Figure 9: Examples for Endocrinology.

Gastroenterology

Question: A 45-year-old woman developed dyspnea with fever over the past week. Sputum culture grows *Streptococcus pneumoniae* and a chest radiograph shows extensive infiltrates of the right lower lobe and a nodule with air-fluid level. Her serum AST is 277 U/L and ALT 183 U/L. This is the gross appearance of her liver. Which of the following is most likely to produce this appearance of her liver?

A) Hepatitis A infection
B) Colonic adenocarcinoma
C) Chronic alcohol abuse
D) Oral contraceptive use
E) Dominant polycystic kidney disease
F) Alpha-1-antitrypsin deficiency

Standard Answer: C) Chronic alcohol abuse



Question: A 27-year-old man has had a chronic diarrhea with weight loss of 5 kg over the past year. On physical examination there are no abnormal findings. His D-xylose absorption is abnormally low. He has elevated anti-endomysial and anti-transglutaminase antibody titers. A jejunal biopsy is performed and shown here in the right panel (compared to the normal jejunum in the left panel). He improves with a change in diet. Which of the following is the most likely diagnosis?

A) Adenocarcinoma
B) Cholera
C) Pseudomembranous enteritis
D) Celiac disease
E) Carcinoid tumor
F) Whipple disease

Standard Answer: D) Celiac disease

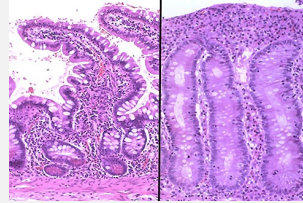


Figure 10: Examples for Gastroenterology.

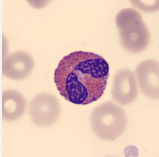
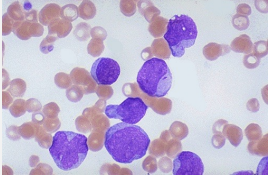
G Evaluation Metrics.

Asclepius comprises a variety of question types, including multiple-choice, yes/no, open-ended questions, and report generation tasks. For multiple-choice and yes/no questions, we use accuracy as the evaluation metric. Open-ended questions require a more nuanced assessment, so we employ GPT to evaluate the precision of the textual responses. The following prompt is used to determine the correctness of an answer:

You are an AI assistant who will help me evaluate responses given the questions and the correct answers. To assess a response, you should provide a single integer score like 0 or 1. A score of 0 indicates that the response is entirely different from answers. A score of 1 indicates that the response aligns perfectly with the answer or is correct for the given question and answer. [Question] [An-

swer] [Response] Your mark: For report generation tasks, we utilize the ROUGE-L scoring system to evaluate how closely the generated texts match the gold-standard reports (Wu et al., 2023c; Chen et al., 2024b). When calculating the overall accuracy, we include all question types except for report generation. The overall accuracy is calculated as the ratio of correctly answered questions to the total number of applicable questions in the benchmark.

Hematology

Question: Which group of peripheral blood cells is visible in this image?

a) Neutrophils
b) Eosinophils
c) Basophils
d) Lymphocytes

Standard Answer: b) Eosinophils

Question: A 30-year-old man has noted a progressively worsening cough for one month. On physical examination, a few small lymph nodes are palpable in his axillae, and the tip of the spleen is palpable. Laboratory studies show Hgb 10.2 g/dL, Hct 31.1%, MCV 90 fL, WBC count 67,400/microliter, and platelet count 36,220/microliter. His peripheral blood smear is shown here. Which of the following is the most likely diagnosis?

A) Acute myelogenous leukemia
B) Plasma cell leukemia
C) Chronic lymphocytic leukemia
D) Acute lymphoblastic leukemia
E) Hairy cell leukemia
F) Leukoerythroblastosis

Standard Answer: A) Acute myelogenous leukemia

Figure 11: Examples for Hematology.

Table 4: **The specialty confidence of each doctor.** Use 1 ~ 5 to represent the confidence score for each specialty. The larger number means more confidence.

Specialty	Dr. 1	Dr. 2	Dr. 3
Cardiology	2	5	4
Dermatology	5	2	3
Endocrinology	3	4	4
Gastroenterology	4	4	4
General Surgery	4	3	4
Hematology	2	4	3
Immunology	5	4	4
Neurology	4	4	4
Obstetrics and Gynecology	2	2	3
Ophthalmology	5	2	5
Orthopedics	4	3	4
Otolaryngology	3	2	3
Pathology	4	2	3
Pulmonology	2	4	4
Urology	4	3	4

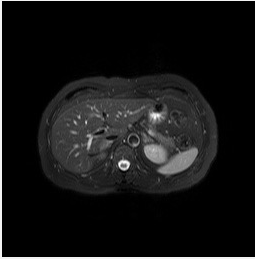
Table 5: Comparison of different MLLMs. The parameters of GPT-4V, GPT-4o, Gemini, and Claude 3.5 Sonnet are estimated to be greater than 100B.

MLLMs	Vision Encoder	LLM	Parameters
GPT-4V	/	/	>100B
GPT-4o	/	/	>100B
Gemini	/	/	>100B
Claude 3.5 Sonnet	/	/	>100B
Med-Flamingo	ViT-L/14	LLaMA	8.3B
RadFM	ViT-3D	LLaMA	14B
XrayGPT	MedClip	Vicuna	7B
CheXagent	EVA-CLIP	Mistral	7B
BiomedGPT-B	BERT	GPT-3	182M

Table 6: The prompt we used to test different MLLMs.

Med-MLLMs	Prompt
GPT-4v, GPT-4o, Gemini, and Claude 3.5 Sonnet	You are a professional doctor. I will give you a question and one or two images. Please utilize the image given to answer the question as a medical expert would. You should only give the answer and no reason or other information. Question: <question> Image: <image>.
Med-Flamingo	You are a helpful medical assistant. Please answer the following question.
RadFM	<image> [image_tokens] </image> [question]
XrayGPT	You are an experienced Doctor, give the following medical scan: ImageContent You will be able to see the medical scan once I provide it to you. Please answer my questions.
CheXagent and BiomedGPT-B	You are a professional doctor. I will give you a question and one or two images. Please utilize the image given to answer the question as a medical expert would.

(a) Case for Anatomical Perception



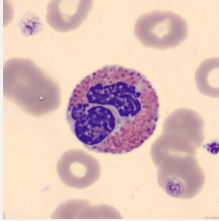
Question: What is the largest organ in the picture?

Standard Answer: Liver

Model Output:

- 1) **GPT-4V:** The largest organ in this MRI image appears to be the liver. ✓
- 2) **Gemini:** The liver. ✓
- 3) **CheXagent:** The largest organ in the picture is the heart. ✗
- 4) **RadFM:** Liver. ✓
- 5) **Med-Flamingo:** Liver. The largest organ in the picture is the liver. The liver is the largest organ in the body. It is located in the upper-right abdominal cavity. It is the largest organ in the body and is the second largest organ in the body. It is the largest organ in the body. ✓
- 6) **XrayGPT:** The large organ that is visible in the picture is the stomach. It appears that there are two ultrasound images of the stomach in the picture, but it is not clear whether they are real or are part of an imaging test. If you can provide more information about the patient and the specific location of the ultrasound images, I can try to give you a more detailed answer. Hope this answers your question. If you have any further questions, please feel free to write. ✗

(b) Case for Attribute Perception



Question: Select the group that best describes the peripheral blood cell image:

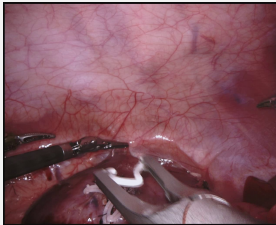
- a) Lymphocytes
- b) Monocytes
- c) Platelets
- d) Basophils

Standard Answer: a

Model Output:

- 1) **GPT-4V:** b) Monocytes ✗
- 2) **Gemini:** b) Monocytes ✗
- 3) **CheXagent:** b) Monocytes ✗
- 4) **RadFM:** a) Lymphocytes ✓
- 5) **Med-Flamingo:** a) Lymphocytes ✓
- 6) **XrayGPT:** c) Platelets ✗

(c) Case for Spatial and Quantitative Perception



Question: Where is monopolar_curved_scissors located?

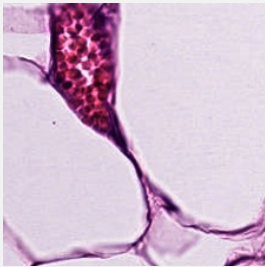
Standard Answer: bottom

Model Output:

- 1) **GPT-4V:** The monopolar curved scissors are located at the bottom right of the image, with black and silver handles and tips pointing to the left side of the image. ✓
- 2) **Gemini:** The monopolar curved scissors are located on the left side of the image. ✗
- 3) **CheXagent:** The monopolar curved scissors is located at the distal end of the esophagus. ✗
- 4) **RadFM:** Proximal. ✗
- 5) **Med-Flamingo:** In the right lower quadrant. ✗ Image 10.1. 10.1 Monopolar Curved Scissors 10.1.1 Indications • Dissection of the colon and rectum. ✗
- 6) **XrayGPT:** Hi, the monopolar curved scissors are used for cutting off excess fluid that is collected in the pleural cavity. This can be caused due to an infection in the lungs. The fluid may also be due to accumulation in the sacs, called pericardium. The fluid in the pericardium is usually not a cause of concern. However, if there is too much fluid in the pericardium it can compress the heart leading to dysfunction. In some cases it can even lead to cardiac rupture. Therefore, a Chest X-ray is done to rule out any fluid collection. Hope I have answered your query. Let me know if I can assist you further. ✗

Figure 12: Case study for perception.

(a) Case for Disease Identification



Question: Does the image show Cancer-associated Stroma (STR)?

Standard Answer: No

Model Output:

- 1) **GPT-4V:** I will review the image you've uploaded to determine if it shows Cancer-associated Stroma (STR). Let's proceed to examine the image. No, the image does not show Cancer-associated Stroma (STR). ✓
- 2) **Gemini:** Yes ✗
- 3) **CheXagent:** No ✓
- 4) **RadFM:** no ✗
- 5) **Med-Flamingo:** Yes ✗
- 6) **XrayGPT:** Hi, the image shows STR and a proliferation of stroma cells that are associated with malignant growth and are responsible for its development and maintenance. Stroma cells are cells that encapsulate and protect growing tumor cells, and are thought to be responsible for the initiation and proliferation of cancer. A variety of stroma cells with a variety of functions have been identified and described. ✗

(b) Case for Spatial and Staging Assessment



Question: What is the severity level of diabetic retinopathy in this retinal fundus image?

- a) Level 0
- b) Level 1
- c) Level 2
- d) Level 3

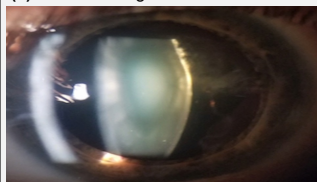
Standard Answer: a

Model Output:

- 1) **GPT-4V:** a) Level 0 ✓
- 2) **Gemini:** c) Level 2 ✗
- 3) **CheXagent:** b) Level 1 ✗
- 4) **RadFM:** a) Level 0 ✓
- 5) **Med-Flamingo:** c) Level 2 ✗
- 6) **XrayGPT:** a) Level 0 ✓

Figure 13: Case study for diagnosis.

(a) Case for Prognosis



Question: A 42-year-old patient is referred for recurrent erosion syndrome after several bouts of painful epithelial erosion. His refraction has been changing. His anterior segment photo is provided. Which is most likely true about his refraction?

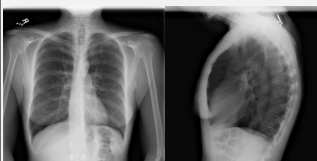
- a) It will likely stabilize without any surgery if the corneal epithelium stops eroding.
- b) It will likely get progressively hyperopic without any surgery.
- c) It will likely get progressively myopic without any surgery.
- d) Central photo therapeutic keratectomy (PTK), if performed, should contribute to further myopia.

Standard Answer: c

Model Output:

- 1) **GPT-4v:** a) It will likely stabilize without any surgery if the corneal epithelium stops eroding. ✗
- 2) **Gemini:** b) It will likely get progressively hyperopic without any surgery. ✗
- 3) **CheXagent:** c) It will likely get progressively myopic without any surgery. ✓
- 4) **RadFM:** His refraction has been changing. His anterior segment photo is provided. ✗
- 5) **Med-Flamingo:** a. 10. A 42-year-old patient is referred for recurrent erosion syndrome after several bouts of painful epithelial erosion. His refraction has been changing. His anterior segment photo is provided. Which is most likely true about his refraction? ✗
- 6) **XrayGPT:** Hello, I have studied your case and would recommend a detailed eye examination. The best treatment for your condition will be to take a close look at your cornea and prescribe you the right lenses. If you do not have any vision loss then you need not worry much. A change in refraction can happen in patients with long term use of certain types of contact lenses. So please take care of your lenses and get them checked for any scratches or dirt. If you have any visual impairment then you need to correct the same as soon as possible. Hope this answers your query. If you have additional questions or follow-up queries then please do not hesitate in writing to us. I will be happy to answer your queries. Wishing you good health. Take care ✗

(h) Case for Report Generation



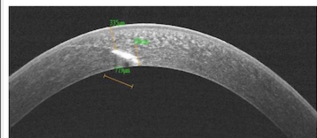
Question: Generate free-text radiology reports for the entered chest X-ray images.

Standard Answer: a

Model Output:

- 1) **GPT-4v:** The cardiomeastinal silhouette is normal in size and contour. The lungs are clear bilaterally without any evidence of focal airspace disease, pleural effusion, or pneumothorax. The bony structures and soft tissues are unremarkable. There is no evidence of anterior or posterior mediastinal widening. The lung fields are clear without any evidence of consolidation or mass. No pleural effusions or pneumothoraces are seen. The bony structures are intact without acute abnormalities. (R-L: 0.235)
- 2) **Gemini:** No obvious acute cardiopulmonary process. (R-L: 0.074)
- 3) **CheXagent:** No acute cardiopulmonary process. (R-L: 0.077)
- 4) **RadFM:** The system does not provide a specific interpretation or diagnosis. The physician can browse through a series of chest X-ray images and select one that best represents the patient's current condition. The physician can also provide her own description of the X-ray findings. (R-L: 0.036)
- 5) **Med-Flamingo:** The chest X-ray image shows a normal cardiac silhouette. The lungs are clear. The heart size is normal. (R-L: 0.216)
- 6) **XrayGPT:** The radiology reports can be generated in minutes. Get an instant PDF or HTML output. No software required. Get your radiology reports today with our online radiology services. Get the best radiology reports with our affordable online services. Our reports can be customized to meet your specific requirements. Contact us today to get the best online radiology services. (R-L: 0.034)

(g) Case Failed Prognosis



Question: A 41-year-old patient with a refraction of -4.00 diopters sphere OU desires refractive surgery. He reports an eye injury from cutting ceramic tile 10 years ago. The eye is normal other than a sliver of white foreign body in the posterior, paracentral cornea. The foreign body is 719 um long, and there are 335 microns between the epithelium and anterior point of the foreign body. Descemet's is intact. Which method of refractive surgery would be the best option?

- a) PRK
- b) LASIK
- c) SMILE
- d) Femtosecond laser-assisted refractive lens exchange

Standard Answer: a

Model Output:

- 1) **GPT-4v:** a) PRK ✓
- 2) **Gemini:** b) LASIK ✗
- 3) **CheXagent:** b) LASIK ✗
- 4) **RadFM:** (FS-LARS) would be the best option. ✗
- 5) **Med-Flamingo:** a) PRK 1. The patient has a history of a foreign body in the cornea. ✓
- 6) **XrayGPT:** Hello, Since there is a foreign body lodged in the cornea, PRK and LASIK are out of the question. A femtosecond laser should be used to remove the foreign body in the posterior and paracentral region of the cornea. Then SMILE can be done for the rest of the cornea. Hope I have answered your query. Let me know if I can assist you further. ✗

Figure 14: Case study for planning. R-L represents the ROUGE-L score.

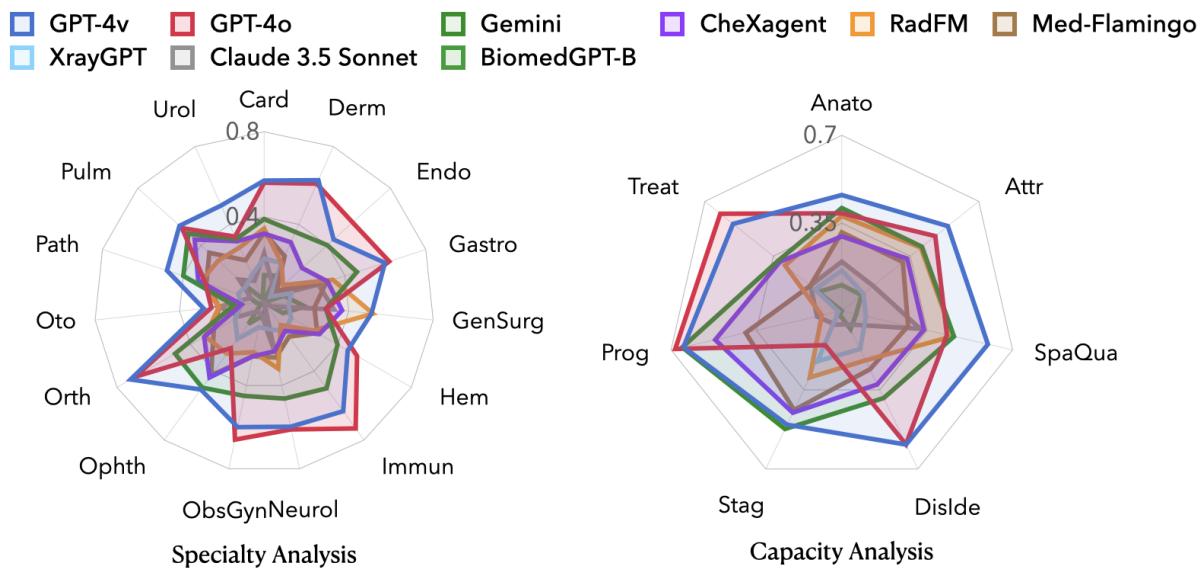


Figure 15: Comparison of Med-MLLMs on our benchmark.

Table 7: Accuracy of models across different specialties.

Model	Card	Derm	Endo	Gastro	GenSurg	Hem	Immun	Neurol
Doctor1	0.636	0.711	0.500	0.542	0.500	0.600	0.483	0.450
Doctor2	0.714	0.400	0.462	0.647	0.450	0.500	0.379	0.560
Doctor3	0.600	0.375	0.800	0.571	0.550	0.400	0.481	0.350
Meta-Doctor	0.674	0.662	0.486	0.764	0.638	0.627	0.557	0.625
GPT-4V	0.571	0.627	0.440	0.598	0.508	0.454	0.633	0.598
GPT-4o	0.561	0.609	0.560	0.619	0.292	0.505	0.733	0.611
Gemini	0.390	0.361	0.400	0.459	0.292	0.399	0.500	0.463
CheXagent	0.322	0.308	0.240	0.314	0.369	0.300	0.167	0.236
RadFM	0.346	0.201	0.120	0.340	0.515	0.267	0.133	0.319
Med-Flamingo	0.327	0.237	0.080	0.309	0.238	0.289	0.200	0.266
XrayGPT	0.205	0.201	0.040	0.134	0.115	0.147	0.167	0.131
Claude3.5Sonnet	0.229	0.095	0.040	0.268	0.331	0.040	0.000	0.240
BiomedGPT-B	0.127	0.136	0.000	0.098	0.192	0.103	0.000	0.035

Model	ObsGyn	Ophth	Orth	Oto	Path	Pulm	Urol	Avg	Var
Doctor1	0.455	0.800	0.423	0.800	0.474	0.500	0.636	0.574	0.014
Doctor2	0.500	0.846	0.500	0.286	0.333	0.500	0.750	0.538	0.023
Doctor3	0.750	0.737	0.500	0.500	0.400	0.600	0.722	0.578	0.020
Meta-Doctor	0.667	0.756	0.600	0.448	0.581	0.689	0.700	0.641	0.007
GPT-4V	0.600	0.507	0.726	0.286	0.481	0.536	0.497	0.543	0.010
GPT-4o	0.660	0.267	0.700	0.250	0.291	0.520	0.337	0.477	0.026
Gemini	0.450	0.496	0.484	0.143	0.400	0.480	0.325	0.428	0.008
CheXagent	0.260	0.437	0.326	0.107	0.326	0.440	0.313	0.343	0.007
RadFM	0.240	0.299	0.321	0.214	0.314	0.291	0.282	0.302	0.009
Med-Flamingo	0.260	0.425	0.274	0.214	0.286	0.347	0.215	0.302	0.006
XrayGPT	0.120	0.214	0.158	0.107	0.128	0.113	0.141	0.148	0.002
Claude3.5Sonnet	0.060	0.053	0.132	0.214	0.067	0.158	0.110	0.136	0.009
BiomedGPT-B	0.070	0.126	0.016	0.036	0.072	0.104	0.018	0.090	0.003